# Specific sorting of the a1 isoform of the V-H$^+$ATPase a subunit to nerve terminals where it associates with both synaptic vesicles and the presynaptic plasma membrane

**Nicolas Morel[1,*], Jean-Claude Dedieu[2] and Jean-Marc Philippe[1,‡]**

[1]Laboratoire de Neurobiologie Cellulaire et Moléculaire, CNRS, 91198 Gif sur Yvette, France
[2]Centre de Génétique Moléculaire, CNRS, 91198 Gif sur Yvette, France
*Author for correspondence (e-mail: nicolas.morel@nbcm.cnrs-gif.fr)
‡Present address: Laboratoire de Génétique et Physiologie du Développement, IBDM, CNRS, 13288 Marseille Cedex 9, France

*Accepted 22 July 2003*
*Journal of Cell Science 116, 4751-4762 © 2003 The Company of Biologists Ltd*
*doi:10.1242/jcs.00791*

## Summary

**Vacuolar H$^+$ATPase (V-ATPase) accumulates protons inside various intracellular organelles, generating the electrochemical proton gradient required for many vital cellular processes. V-ATPase is a complex enzyme with many subunits that are organized into two domains. The membrane domain that translocates protons contains a proteolipid oligomer of several c subunits and a 100 kDa a subunit. Several a-subunit isoforms have been described that are important for tissue specificity and targeting to different membrane compartments, and could also result in the generation of V-ATPases with different functional properties. In the present report, we have cloned the *Torpedo marmorata* a1 isoform. This isoform was found to be addressed specifically to nerve endings, whereas V-ATPases in the neuron cell bodies contain a different a-subunit isoform. In nerve terminals, the V-ATPase membrane domain is present not only in synaptic vesicles but also in the presynaptic plasma membrane, where its density could reach 200 molecules μm$^{-2}$. This V-ATPase interacts with VAMP-2 and with the SNARE complexes involved in synaptic vesicle docking and exocytosis.**

Key words: V-ATPase, SNARE complex, Freeze-fracture, Fusion pore

## Introduction

Vacuolar H$^+$-ATPases (V-ATPases) translocate protons across the membrane of various organelles (lysosomes, endosomes, trans-Golgi cisternae, secretory granules etc.), creating an electrochemical proton gradient that is acidic and positive within these intracellular compartments (Stevens and Forgac, 1997; Nelson and Harvey, 1999; Nishi and Forgac, 2002; Schoonderwoert and Martens, 2001). Acidification of these organelles is required for many cellular processes (maturation and processing of proteins, receptor-mediated endocytosis, coupled intracellular transport of small molecules, etc.). V-ATPases are also present in specialized domains of the plasma membrane of certain proton-secreting cells such as osteoclasts, macrophages and renal intercalated cells (Nelson and Harvey, 1999; Nishi and Forgac, 2002).

V-ATPases are large multimeric enzymes, made up of several different subunits. These subunits are organized into two domains, a cytoplasmic domain V1 that hydrolyses ATP and a membrane domain V0 involved in proton translocation. The V1 catalytic domain (~600 kDa) is composed of eight different subunits (A-H) with three copies of the nucleotide-binding subunits A and B. The membrane V0 domain (250 kDa) contains five or six proteolipid subunits c (and c′) and single copies of subunits a, d and c′ (Nishi and Forgac, 2002; Nelson and Harvey, 1999). The a subunit of the V0 domain is a 100 kDa integral membrane protein containing nine transmembrane helices in its C-terminal half, with a large N-terminal sector in the cytoplasm (Leng et al., 1999). Multiple isoforms of the a subunit have been identified, with specific organelle or cellular distributions. In yeast, the two a isoforms (Vph1p and Stv1p) are associated with vacuolar and Golgi/endosomal membranes, respectively (Manolson et al., 1994; Kawasaki-Nishi et al., 2001). In mice, four different isoforms have been described (a1-a4), encoded by different genes with tissue-specific expression (Toyomura et al., 2000; Nishi and Forgac, 2000; Oka et al., 2001). The diversity of the a-subunit isoforms is not only important for tissue specificity and targeting to different membrane compartments; it could also result in the generation of V-ATPases with different functional properties (Kawasaki-Nishi et al., 2001). In contrast to the a subunit, other subunits of the membrane domain of vertebrate V-ATPases are encoded by single genes (Nishi and Forgac, 2002).

In neurons, V-ATPases are also present in the membrane of synaptic vesicles, the neurotransmitter-storing organelles (Stadler and Tsukita, 1984; Hicks and Parsons, 1992). The large electrochemical H$^+$ gradient generated by this enzyme [pH 5.2-5.5 inside the synaptic vesicles (Michaelson and Angel, 1980; Füldner and Stadler, 1982)] is used by specific vesicular transporters to accumulate the neurotransmitter. In addition to this well established role in neurotransmitter storage, V-ATPase could also participate in the constitution of

a fusion pore involved in neurotransmitter release (Morel et al., 2001) and membrane fusion (Peters et al., 2001).

In the present work, we have cloned a neuron specific isoform of the V-ATPase a subunit and studied its subcellular distribution in electromotoneurons from the fish *Torpedo marmorata*. This homogeneous population of neurons, which innervate the electric organs, allows the characterization of V-ATPases in two functionally different neuronal compartments: the somatodendritic and nerve terminal compartments (Morel et al., 1998). Electromotoneuron cell bodies (120 μm in diameter) and dendrites are located in the electric lobes, a well identified portion of the *T. marmorata* brain that contain no other neurons, and are only contacted by very few nerve endings (Roberts and Ryan, 1975). Electromotoneuron nerve terminals can be isolated from the electric organs to give very pure fractions of functional synaptosomes (Morel et al., 1977). This neuron-specific isoform of the V-ATPase a subunit is addressed to the nerve terminal compartment, where it is present both in synaptic vesicles and in the presynaptic plasma membrane. The membrane domain of nerve terminal V-ATPase interacts with SNARE complexes, which have been shown to be involved in synaptic vesicle docking and exocytosis (Jahn and Südhof, 1999; Chen and Scheller, 2001).

## Materials and Methods

### Antibodies

Monoclonal antibodies (mAbs) prepared in the laboratory: mAb 15K1 to the V-ATPase c subunit (Morel et al., 1991); mAb 19K2 to VAMP/synaptobrevin-2 (Taubenblatt et al., 1999); and mAb 1567 obtained after mouse immunization with SNARE complexes (Shiff et al., 1996). Syntaxin-1 was detected using mAb HPC-1 (Sigma) and the V-ATPase B subunit with monoclonal antibody 2E7 (gift from H. Sze). To detect the V-ATPase A subunit, we raised a rabbit antiserum to the C-terminal peptide KEDMQNAFRSLED linked by glutaraldehyde to key-hole limpet hemocyanin. For V-ATPase a1-subunit detection, we prepared a rabbit antiserum to the C-terminal peptide FSFESILEGRFEE, cross-linked to bovine serum albumin (BSA) via an added N-terminal cysteine. Affinity-purified antibodies to the a1 subunit were obtained after binding to the same peptide, cross-linked via the cysteine to a UltraLink Iodo acetyl gel (Pierce). A rabbit antiserum to synaptophysin was raised against a synthetic peptide (EQEGYQPNYGQ) cross-linked to BSA by glutaraldehyde. For detection of SNAP-25, a rabbit antiserum from the laboratory was used (Taubenblatt et al., 1999). All synthetic peptides and conjugates used for immunizations were from Neosystem (France).

### Molecular cloning of *T. marmorata* subunit a1

Poly(A)$^+$ RNAs extracted from *T. marmorata* electric lobes and a *T. marmorata* electric lobe cDNA library constructed in λZAPII were kindly provided to us by F. M. Meunier (Birman et al., 1990). cDNAs were generated by oligo-dT-primed reverse transcription of electric lobe poly(A)$^+$ RNAs (Mo-MLV-RNAse H$^-$ reverse transcriptase from Promega). Degenerate primers were designed that correspond to two conserved amino acid sequence stretches found in all V-ATPase a-subunit isoforms, from mouse to *Caenorhabditis elegans* ($_{740}$YLRLW with an added *Eco*RI 5′ extension for the a-cons-S1 forward primer and $_{795}$MEGLS with a *Cla*I 5′ extension for the a-cons-AS1 reverse primer). Using these primers and *T. marmorata* electric lobe cDNAs as template, V-ATPase a-subunit partial cDNAs were amplified by PCR. After purification in agarose gels, 200 base-pair PCR products were inserted in BlueScript II SK$^-$ plasmid and cloned using electrocompetent XL1-blue *Escherichia coli*. The inserts of clones selected by PCR were sequenced (MWG-Biotech). Forward 3T3-S1 and 3T3-S2 nested internal primers, specific for this *T. marmorata* a-subunit sequence, were used in association with a reverse λZAP-derived T7 primer to amplify by PCR, from the *T. marmorata* electric lobe cDNA library, 600 base-pair cDNAs encoding the 3′ end sequence of V-ATPase a subunit. They were inserted in pGEM-T-easy plasmids, cloned in XL1-blue *E. coli* and sequenced. The 5′ end sequence (2.8 kb) was determined using the SMART IIA-5′ RACE kit (Clontech) with *T. marmorata* a1-subunit-specific nested reverse primers, a1-AS1 and a1-AS2. All primers were obtained from MWG-Biotech.

### Subcellular fractionation

*T. marmorata* fishes were provided by the Marine Station of Roscoff, France. Isolated nerve terminals (synaptosomes) were prepared from the *T. marmorata* electric organ as described previously (Morel et al., 1977).

Nerve terminal plasma membranes were isolated after biotinylation of intact synaptosomes essentially as described (Taubenblatt et al., 1999). Synaptosomes in suspension in *T. marmorata* physiological medium (Morel et al., 1977) were incubated for 90 minutes at 6°C with Sulfo-NHS-lc-Biotin (UP54398A, Interchim, at 0.9 mM final concentration). Free biotin was then quenched by a 15 minute incubation after addition of Tris buffer pH 7.5 (50 mM final concentration). Synaptosomes were then concentrated by centrifugation [10,000 ***g*** (max) for 20 minutes] and the synaptosomal pellet was carefully surface-washed to remove unbound biotin. Synaptosomes were disrupted by resuspension [1 (mg protein) ml$^{-1}$] in a hypoosmotic buffer [10 mM Tris buffer pH 7.0, 1 mM EDTA, protease inhibitor cocktail (P8340, Sigma, 1 μl ml$^{-1}$)], freezing in liquid nitrogen and powdering in a mortar while frozen. Membranes in the thawed sample were pelleted [180,000 ***g*** (max) for 40 min], resuspended in PBS (150 mM NaCl, 10 mM Na phosphate buffer, pH 7.4) and isolated on streptavidin-coated magnetic beads (Dynabeads M280, Dynal). After several washes of the beads in PBS, antigens in bound membranes were directly solubilized in SDS cracking buffer. As a control, non-biotinylated synaptosomes were fractionated in parallel.

Synaptic vesicles were purified from frozen *T. marmorata* electric organs by fractionation in two successive sucrose gradients as reported by Diebler and Lazereg (Diebler and Lazereg, 1985).

### Immunoprecipitation of SNARE complexes

Monoclonal antibodies to VAMP-2 (mAb 19K2), syntaxin-1 (Cl HPC-1) and SNARE complexes (mAb 1567) were covalently bound to anti-mouse IgG-agarose beads (Sigma, A6531) using dimethylpimelimidate (Pierce). They were incubated in PBS containing 2% (w/v) BSA and washed in PBS before use. Synaptosomes or electric lobe homogenates were solubilized [0.5 (mg protein) ml$^{-1}$ in PBS] by CHAPS (30 mM) for 30 minutes on ice. Unsolubilized proteins were removed by centrifugation [180,000 ***g*** (max) for 60 minutes]. Solubilized proteins in the supernatant were directly incubated with the antibody coated beads in suspension in PBS for 5 hours at 6°C [0.2 (mg protein) ml$^{-1}$ and 10 mM CHAPS final dilutions]. Unbound proteins (nr samples) were recovered in the supernatant after gentle spinning of beads, pooled with the first PBS (containing 10 mM CHAPS) wash. Beads were extensively washed in PBS (+ 10 mM CHAPS) and immunoprecipitated antigens (ip samples) were recovered after elution by 1% SDS in 0.1 M $Na_2CO_3$. Synaptosomal proteins in the mAb 19K2 and HPC1 nr samples (depleted of VAMP-2 and syntaxin-1, respectively, and also of SNARE complexes) were submitted to a second incubation with mAb-coated beads (1567, HPC-1 and 19K2), under similar conditions. An aliquot of solubilized synaptosomal proteins, NR and ip samples were extensively dialysed against 0.05% SDS at room temperature, and concentrated under vacuum (Speedvac).

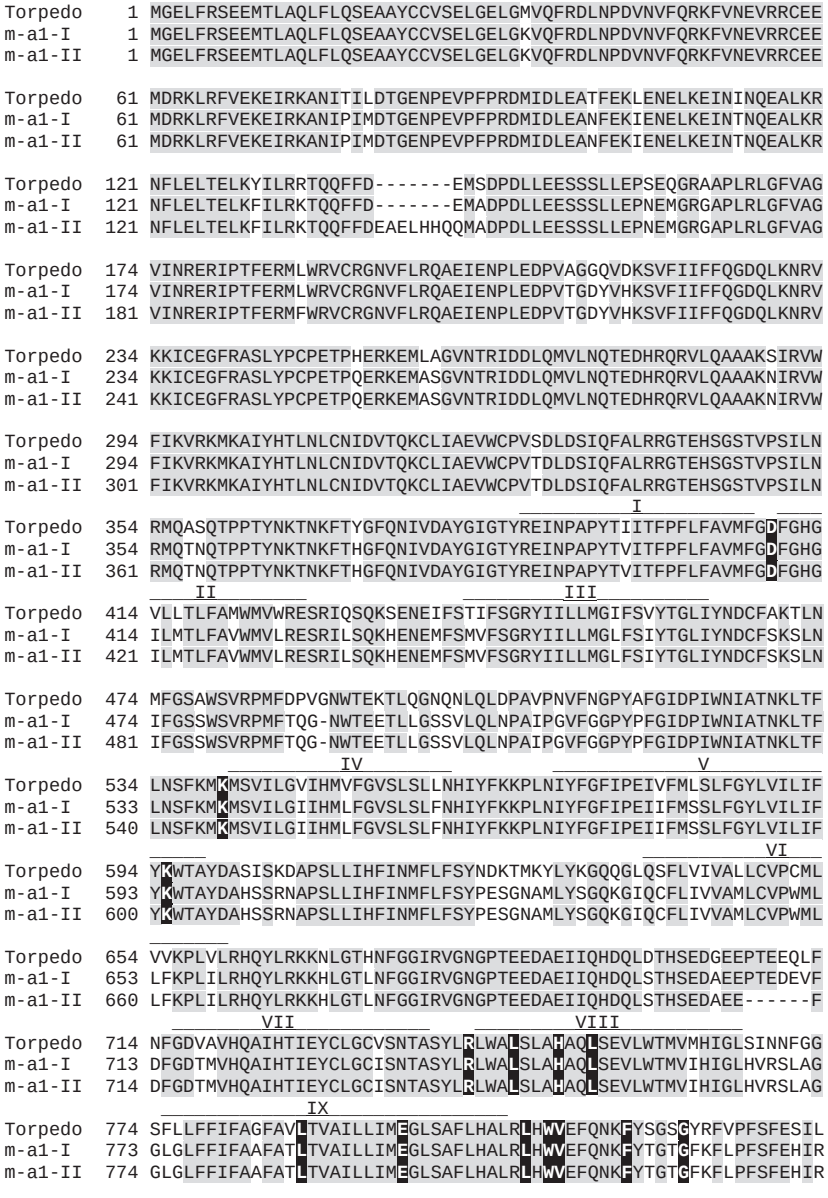

**Fig. 1.** Amino acid sequence alignment of the *T. marmorata* and mouse a1 isoforms of the V-ATPase a subunit. The *T. marmorata* sequence obtained in the present report was compared with the sequences of two splice variants (a1-I and a1-II) of the mouse a1 isoform of the V-ATPase a subunit (Nishi and Forgac, 2000). Identical residues are shaded in grey. The nine putative transmembrane domains assigned in the yeast homologue Vph1 (Leng et al., 1999) are shown with a dark bar (I to IX). Conserved residues whose mutation affects the activity or assembly of yeast V-ATPase are in black (Leng et al., 1998).

### Immunofluorescence

Pieces of tissue were fixed in 4% paraformaldehyde (in 40 mM Na phosphate buffer, 5 mM EDTA, 30% sucrose, pH 7.4) for 7 hours. Tissue blocks were frozen in isopentane cooled by liquid nitrogen. Sections (10 μm thick) were mounted on gelatine-coated slides and stored at –70°C. Before immunostaining, tissue sections were treated by 0.5% SDS in 0.4 M Tris buffer pH 7.4 for 40 minutes at room temperature, rinsed in TBS (0.4 M NaCl, 20 mM Tris buffer, 0.1% Tween 20, pH 7.4) and incubated for at least 1 hour in TBS containing 1% BSA and 1% sheep serum. All antibodies were diluted in TBS containing 1% sheep serum and 1% BSA, and, after 30 minutes, centrifuged for 10 minutes at 12,000 ***g***. Sections were incubated overnight with primary antibodies, extensively washed in TBS and reincubated with secondary antibodies (5 hours). After several washes in TBS, sections were mounted in Vectashield (Vector) with glass coverslips and stored at 4°C.

### Freeze-fracture immunolabelling

Small pieces of *T. marmorata* electric organ were preincubated in calcium-free *T. marmorata* physiological medium. Synaptosomes were concentrated [about 50 (mg protein) $ml^{-1}$] by centrifugation [10,000 ***g*** (max) for 20 minutes]. They were ultra-rapidly frozen, and freeze-fractured by the 'sandwich freezing' procedure (Gulik-Krzywicki and Costello, 1978); the fractured surface was replicated as previously described (Taubenblatt et al., 1999) and the membrane antigens adsorbed to the replicas were detected according to Fujimoto (Fujimoto, 1995) as adapted by Taubenblatt et al. (Taubenblatt et al., 1999).

### Other methods

Protein was measured by the Lowry method. Antigens were detected and quantified after SDS solubilization, electrophoresis in acrylamide gels, electrotransfer onto nitrocellulose blots that were probed with specific antibodies. Their binding was indirectly visualized by peroxidase-conjugated anti-IgG antibodies and chemiluminescent detection (ECL, Amersham). Band intensities were quantified with a densitometer (Perfect Image, Claravision) and antigen contents quantitated by comparison with increasing amounts of a synaptosomal fraction treated in the same gels.

## Results

### Cloning of the a1 subunit of *T. marmorata* V-ATPase

The amino acid sequence of the V-ATPase a subunit has been determined in many organisms and, for several of them, multiple isoforms have been identified. After comparison of many of these sequences, we identified two amino acid sequence stretches that are conserved throughout the different organisms and in the different isoforms of the a subunit. These conserved stretches contain amino acid residues that were shown to be functionally important and extend in the transmembrane domain 8 (amino acids 740 to 750 for mouse a1-I) (Fig. 1) and at the junction of the ninth transmembrane domain and the C-terminal cytoplasmic loop (amino acids 795 to 810) (Leng et al., 1999). Degenerate oligonucleotide primers were designed that correspond to these two amino acid sequence stretches ($_{740}$YLRLW and $_{795}$MEGLS). Using these primers and *T. marmorata* electric lobe cDNAs as template, V-ATPase a-subunit cDNA fragments were amplified by PCR, cloned and sequenced. From this *T. marmorata* sequence, specific forward and reverse nested primers were designed. The 3′ end sequence of mRNAs encoding *T. marmorata* V-ATPase a subunit was determined after PCR amplification, cloning and sequencing, from a *T. marmorata* electric lobe cDNA library

(constructed in the λZAP vector) using *T. marmorata* specific forward primers and a phage-specific reverse oligonucleotide. The 5′ end sequence (2.8 kb) was determined from purified electric lobe mRNAs, using the SMART IIA-5′ RACE kit (Clontech) with *T. marmorata* a-subunit-specific nested reverse primers.

The a-subunit *T. marmorata* cDNA (EMBL accession number AJ555619) encodes a 839 amino acid polypeptide that is closely related to the four V-ATPase a subunits characterized in mouse. Sequence comparisons revealed that *T. marmorata* a subunit is the orthologue of mouse V-ATPase a1-subunit (Fig. 1), showing 76% and 87% identity at the nucleotide and amino acid levels, respectively. Amino acid sequence homology with the other mouse isoforms was much lower (60% identity with the a4 isoform and less than 50% with the a2 and a3 isoforms). Three splice variants of the a1 subunit have been identified in mice that differ in the presence or absence of small exons near the N- or C-termini of the protein (Nishi and Forgac, 2000). The N-terminal exon (seven amino acids long) is present in the a1-II isoform, the C-terminal exon (six amino acids) is specific for the a1-I variant, and subunit a1-III lacks both exons (Nishi and Forgac, 2000). The major form expressed in *T. marmorata* electric lobe corresponds to subunit a1-I (Fig. 1). Using paired primers that allow the specific amplification from *T. marmorata* electric lobe cDNAs of the N-terminal- or C-terminal-exon-containing domains, we detected, in addition to the abundant a1-I transcripts, minor transcripts that either contain the N-terminal exon or do not contain the C-terminal one (not shown). These minor transcripts were cloned and sequenced. The amino acid sequence of the *T. marmorata* a1-subunit N-terminal exon (EAELHHQ, nucleotide sequence: GCTGAATTGCATCATCAGCAG) is identical to its mouse orthologue (a1-II isoform, EMBL accession number AJ555620). It has not been possible to clone other isoforms of the V-ATPase a subunit from *T. marmorata* electric lobe mRNAs.

Subunit a1 of V-ATPase is therefore well conserved between *T. marmorata* and mouse, with preservation of all amino acids whose mutations were shown, in the yeast homologue, to affect V-ATPase activity or association (Leng et al., 1998; Leng et al., 1999).

## Isoform a1 of the a subunit of V-ATPase is neuron-specific and addressed to nerve terminals

We have generated rabbit polyclonal antibodies against the 13-amino-acid long C-terminal peptide of *T. marmorata* V-ATPase subunit a1 (Fig. 1). In mice, the corresponding epitope was shown to be specific for the a1 isoform of the V-ATPase a-subunit (Toyomura et al., 2000; Nishi and Forgac, 2000; Oka et al., 2001). In *T. marmorata* cerebellum frozen sections (Fig. 2A), the antiserum bound to nerve-ending-rich regions. The cerebellum molecular layer was intensely stained and the granular cell layer showed a spotty labelling identical to that obtained with anti-SV2 antibodies, a marker of synaptic vesicles (not shown). The same immunostaining was obtained with affinity-purified antibodies (purified using peptide-coated acrylamide beads). Labelling was no longer detected using antiserum that had been adsorbed on the immunogen-coated beads (Fig. 2A). In parallel experiments, the antibodies against a1, either the antiserum or the affinity-purified antibodies, bound to a single 95 kDa band on western blots of synaptosomal proteins (Fig. 2B). This molecular weight is similar to that reported for the V-ATPase a subunit in other organisms (Nelson and Harvey, 1999; Nishi and Forgac, 2002). Labelling of the 95 kDa band was lost after pre-adsorption of the antiserum on the immunogen (Fig. 2B).

The anti-a1 antibodies were used to compare the subcellular distributions of the V-ATPase a1 and c subunits in *T. marmorata* electromotoneurons. The cell bodies (120 μm in diameter) of these neurons are located in the electric lobes, which contain no other neurons, and are only contacted by very few nerve endings (Roberts and Ryan, 1975). This is apparent in the parasagital section of *T. marmorata* brain at low magnification (Fig. 2C), after immunostaining by a synaptic-vesicle-specific antibody (anti-SV2 antibody). Nerve terminal labelling was visualized in all brain regions, except in the electric lobes, being most intense in the cerebellum molecular layer (Fig. 2C). Nerve endings in the rhombencephalum, below the electric lobe, were labelled by antibodies against both the c and the a1 subunits (Fig. 2D, green and red, respectively). Virtually no labelling by the anti-a1 antibodies was detected in the electric lobe, even though a high level of transcript was detected by in situ hybridization (data not shown). However, the V-ATPase c subunit was detected in intracellular granules in the electromotoneuron cell bodies (Fig. 2D). Therefore, the a1 isoform of V-ATPase a subunit appears to be concentrated in nerve endings, in contrast to the ubiquitous c subunit, which is abundant in both nerve endings and the cell bodies.

Different tissue homogenates were compared for their content of the a1 isoform of the V-ATPase a subunit in immunoblot experiments. The a1 subunit was easily detected in brain but not in liver and kidney homogenates, in spite of the fact that tissue samples contained similar amounts of the V-ATPase c subunit (Fig. 3). Synaptosomes (pure isolated nerve terminals) contained both the a1 and the c subunits, whereas only the c-subunit band was visualized in electric lobe homogenates. Comparing these two samples at equal content of V-ATPase c subunit suggests that the a1 subunit is at least ten times more concentrated in nerve terminals than in electromotoneuron cell bodies and dendrites. The same concentration factor was observed for the nerve terminal SNARE proteins syntaxin-1 and VAMP-2 (Fig. 3). Very pure *T. marmorata* synaptic vesicles contain the V-ATPase a1 and c subunits (Fig. 3). A similar stoichiometry between the a1 and c subunits was found in synaptosomes and in synaptic vesicle preparations. Subunits of the membrane domain of V-ATPase (a1 and c) are less enriched than VAMP in a very pure synaptic vesicle fraction that does not contain detectable amounts of the plasma membrane marker syntaxin-1 (Fig. 3). This suggests that V-ATPase could be present in several membrane compartments in nerve terminals.

## Proteolipid domain of V-ATPase is present both in synaptic vesicles and in the presynaptic membrane

The distribution of the proteolipid domain of V-ATPase in nerve endings was studied in *T. marmorata* electric organ (Fig. 4) and synaptosomes (Fig. 5) using the SDS-digested freeze-fracture replica labelling technique (Fujimoto, 1995; Taubenblatt et al., 1999). Nerve endings, either in situ in the electric organ or in suspension, were rapidly frozen (in less

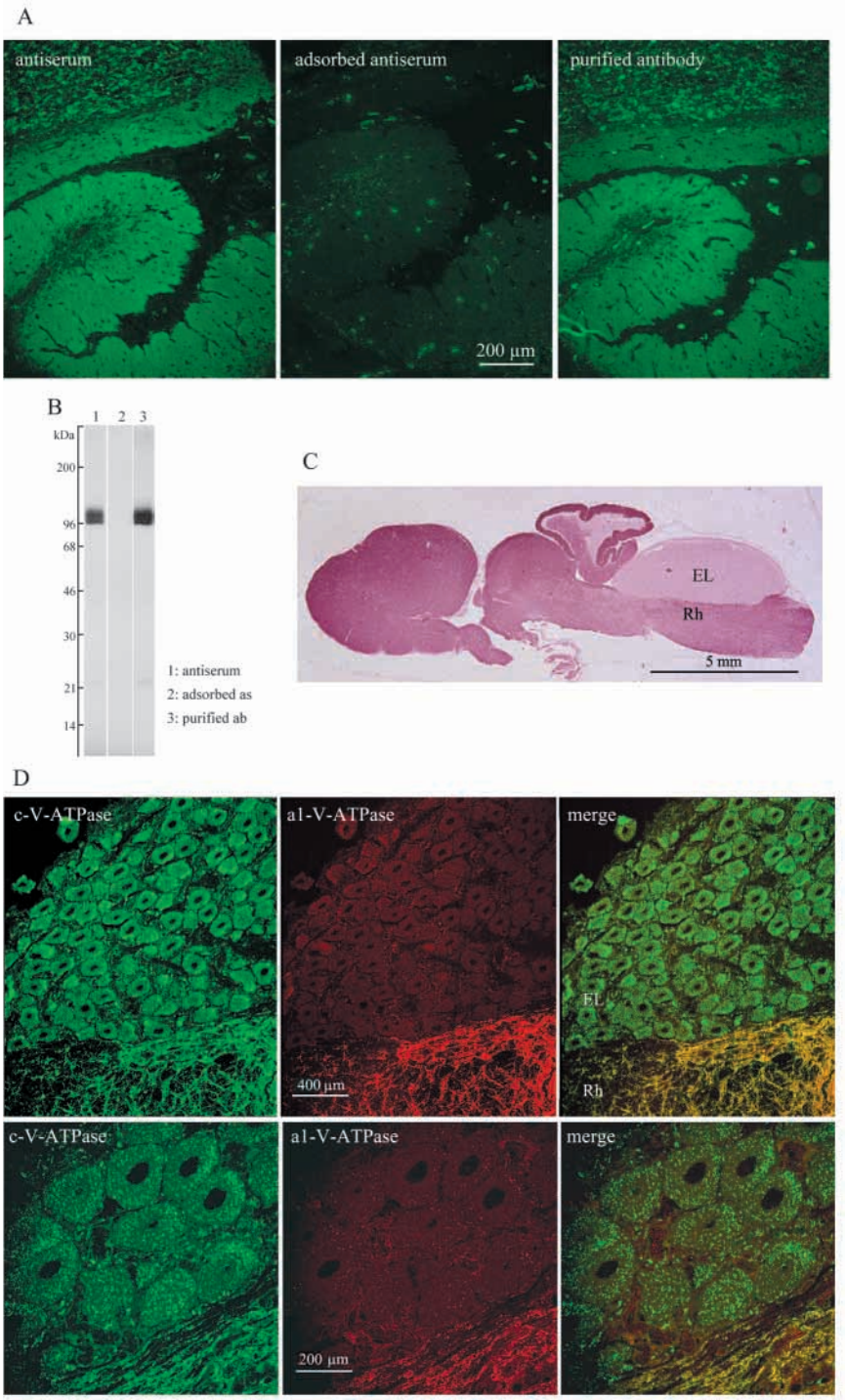


**Fig. 2.** The a1 isoform of the V-ATPase a subunit does not co-localize with the c subunit in neuron cell bodies. A rabbit antiserum was generated by immunization with a synthetic peptide (13 C-terminal amino acids of the a1 isoform of *T. marmorata* V-ATPase subunit a) linked to BSA. Specific anti-a1-isoform antibodies were affinity purified on beads coated with the immunopeptide (purified antibody), whereas the serum fraction that did not bound to the beads corresponds to the adsorbed antiserum. (A) Binding of the anti-a1 antiserum (left), adsorbed antiserum (middle) and purified antibodies (right) on *T. marmorata* cerebellum frozen sections, indirectly visualized with FITC-conjugated anti-rabbit IgG antibodies. Scale bar, 200 μm. (B) Binding of the anti-a1 antiserum (1), adsorbed antiserum (2) and purified antibodies (3) on an immunoblot of synaptosomal proteins (40 μg protein per slot). (C) Distribution of the SV2 synaptic vesicle antigen in a parasagital section of *T. marmorata* brain (indirect immunolabelling by an anti-SV2 antibody, a peroxidase-conjugated anti-mouse Ig antibody and di-amino-benzidine staining). Scale bar, 5 mm. (D) Double staining of the c subunit (green) and a1 isoform of the a subunit (red) of V-ATPase in *T. marmorata* electric lobe frozen sections. Binding of mouse anti-subunit-c and rabbit anti-a1-isoform antibodies was indirectly visualized by anti-mouse or anti-rabbit Ig antibodies conjugated to FITC or Alexa 633, respectively. Right-hand panels (merge) correspond to the superimposed stainings. Scale bars, 400 μm (top row) and 200 μm (bottom row). EL, electric lobe; Rh, rhombencephalum.

than 1 millisecond) in the absence of any chemical fixation or detergent permeabilization. The frozen tissue was fractured and a film of platinum (Pt) and carbon (C) was deposited on the fractured surface. The fracture splits membranes in between the two lipid layers, exposing the hydrophobic surface of either their cytoplasmic (P) or external (E) leaflets. Membrane proteins are pinched off preferentially with the P or E leaflet according to the relative strength of their cytoplasmic or extracellular interactions. The fractured tissue, covered by the Pt/C replica, was allowed to thaw in PBS and was then dissolved with SDS. The membrane protein domains that are exposed after the fracture of membranes are embedded in the Pt/C film. Membrane proteins remain associated with the replica after SDS solubilization, allowing their detection by indirect immunogold labelling. Using this approach on *T. marmorata* nerve terminals, VAMP was visualized in both synaptic vesicles and the presynaptic membrane,whereas syntaxin-1 was detected only in the nerve terminal membrane (Taubenblatt et al., 1999).

In the right-hand part of Fig. 4, the fracture went through the nerve terminal cytoplasm, showing many synaptic vesicles. It then split the presynaptic membrane, exposing a large surface of its external leaflet. The anti-V-ATPase c-subunit antibodies bound both to synaptic vesicles and to the presynaptic membrane, detected by the presence of 15 nm gold particles. These particles were not homogeneously distributed in the presynaptic membrane, being associated with its external leaflet and concentrated in certain areas (Fig. 4). Similar results were obtained on isolated nerve terminals (Fig. 5). When the fracture crosses the cytoplasm, some synaptic vesicles were decorated with gold particles (Fig. 5, right). When the synaptosomal membrane is fractured, most gold particles are associated to its external leaflet (Fig. 5). This shows that V-ATPase c subunit is pinched

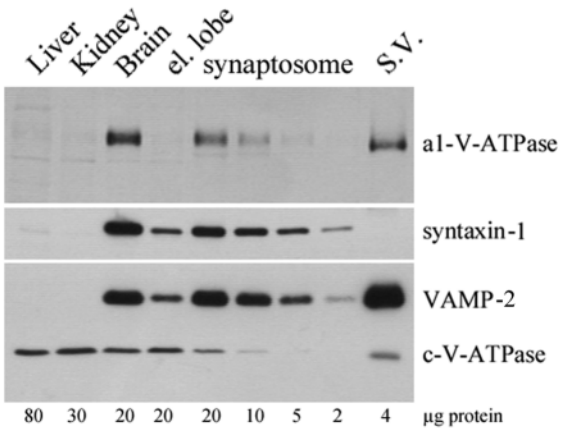


**Fig. 3.** The a1 isoform of the V-ATPase a subunit is concentrated in nerve terminals. The a1-subunit distribution in different tissues (liver, kidney, brain and electric lobe) was studied by western blotting of tissue aliquots containing similar amounts of the V-ATPase c subunit (c-V-ATPase) and compared with the distribution in the same samples of the nerve terminal SNARE proteins VAMP-2 and syntaxin-1. The distribution of these antigens in the somatodendritic (electric lobe) and nerve terminal (synaptosome) compartments of *T. marmorata* electromotoneurons was compared. The protein amount in each sample is indicated (µg protein). SV, purified synaptic vesicles.

off with the external membrane leaflet. The fracture-label technique allows the determination of the transmembrane orientation of the antigens because the Pt/C replica overlaid on the E face fractures masks the cytoplasmic epitopes, and vice versa for the extracellular epitopes and the P-face-associated proteins (see Fujimoto, 1995). The antibody we used (mAb 15K1) binds to the N-terminal ten amino acids of the c subunit, which are therefore exposed on the extracellular surface of the presynaptic membrane or in the lumen of synaptic vesicles.

A quantitative analysis of c-subunit immunolabelling was performed on several different experiments (three and two experiments for in situ nerve terminals and synaptosomes, respectively). Gold particle density associated with E face of in situ nerve terminal membrane was 4.0±2.1 gold particles per $\mu m^2$ (mean±s.e.m. of 30 nerve terminals), ranging from 0 to 8.0 gold particles per $\mu m^2$. Labelling of the synaptosomal membrane E leaflet was 3.9±3.9 gold particles per $\mu m^2$ (mean±s.e.m. of 274 synaptosomes). Labelling of the synaptosomal membrane E face was quite variable, ranging from 0 to 18.1 gold particles per $\mu m^2$. This variability was higher for synaptosomes than for in situ nerve terminals owing to the much larger membrane surface that is fractured in the latter case. It is probably related to the non-homogeneous distribution of the V-ATPase c subunit in the presynaptic membrane (Fig. 4). We have estimated that 5.6% of synaptic vesicle membrane E-face profiles were decorated with a gold particle (4200 synaptic vesicle convex profiles counted). Considering the mean area of a fractured vesicle profile ($6\times10^{-3}$ $\mu m^2$), the gold particle density in synaptic vesicles would be around ten gold particles per $\mu m^2$, two to three times higher than the mean density in the presynaptic membrane. Such a density, given the total surface area of a synaptic vesicle (80 nm diameter, $2\times10^{-2}$ $\mu m^2$ surface area), corresponds to the labelling of about 20% of synaptic vesicles.

Gold particles are observed in the vicinity of large intramembrane particles (IMPs). This is especially apparent on the flat surface of in situ presynaptic membrane E faces (Fig. 6). These particles correspond to large protein structures with several transmembrane domains (Eskandari et al., 1998). We have statistically tested the possibility that gold beads were preferentially associated with large IMPs. We have estimated the density of intramembrane particles in a 20 nm radius large disk, centred on each gold particles, in flat membrane profiles similar to that of Fig. 6. The size of this disk was chosen considering the length of Ig molecules (2×7 nm IgG) and the gold particle diameter (15 nm). We found, in the close vicinity of gold particles, a density of 860 IMPs $\mu m^{-2}$ (from 81 disks in 13 different membrane profiles). This is much higher than the overall mean density of intramembrane particles in the same membrane profiles (236±24 IMPs $\mu m^{-2}$), showing a preferential association of gold label to large intramembrane

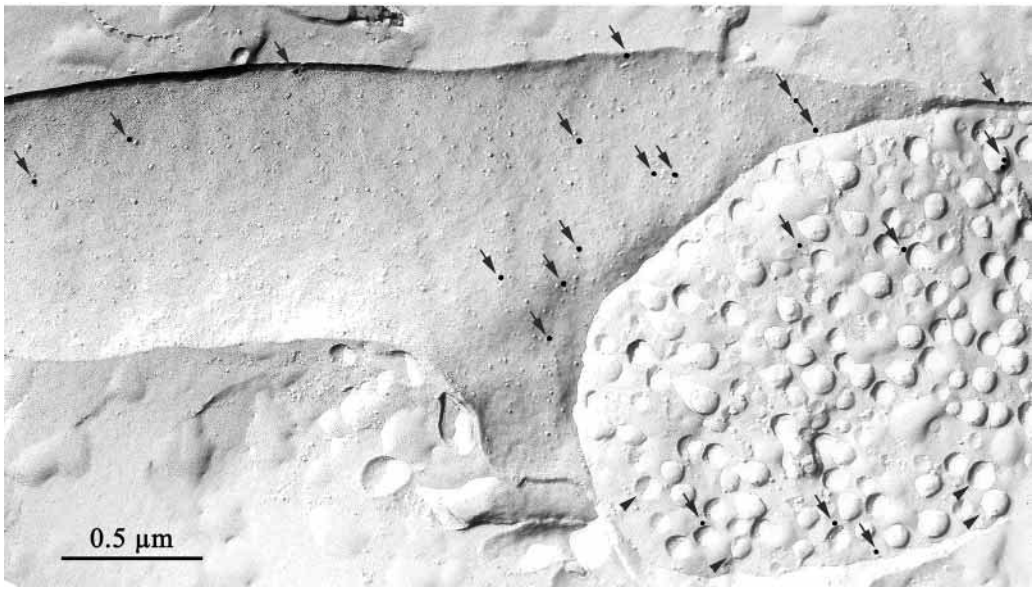


**Fig. 4.** Immunogold detection of the V-ATPase subunit c in a freeze-fractured nerve ending. A typical nerve terminal, frozen in situ in the electric organ, was fractured and replicated. The fracture plane crosses the nerve terminal cytoplasm (right), which contains many synaptic vesicles (arrowheads). It splits the plasma membrane (left), exhibiting a large surface area of the presynaptic membrane E face. Binding of mAb 15K1 to the V-ATPase c subunit embedded in the replica was indirectly visualized using anti-mouse Ig antibodies conjugated to 15 nm gold particles (arrows).

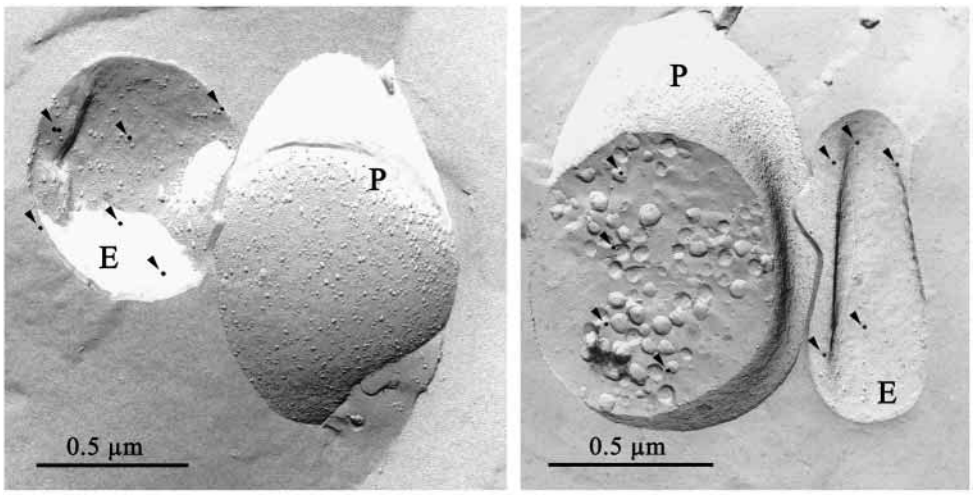


**Fig. 5.** V-ATPase c-subunit distribution in freeze-fractured synaptosomes. Typical freeze-fractured synaptosomal profiles that illustrate the preferential detection of the V-ATPase c subunit in the external leaflet (E) of the synaptosomal membrane. Synaptic vesicles in the synaptosome cytoplasm (right) are also labelled by gold particles (arrowheads). P, cytoplasmic leaflet of the synaptosomal membrane.

particles. This suggests that most of the V-ATPase c subunits exist in the presynaptic membrane as constituents of large protein complexes.

In parallel fracture-label experiments, we tried without success to detect the a1 subunit of the V0 domain of V-ATPase using purified anti-a1 antibodies. These antibodies bind to the C-terminal tail of the a1 subunit (see above), which is oriented in the synaptic vesicle lumen or the extracellular space (Leng et al., 1999). One likely interpretation of these negative results is that this epitope is masked by the Pt/C replica, suggesting that the a1 subunit is pinched off with the membrane P face, independently from the proteolipid oligomer. This could have been expected since the N-terminal moiety of the a-subunits is hydrophilic and cytoplasmic, in interaction with the catalytic V1 sector.

The synaptosomal plasma membrane was isolated and its antigenic content compared with that of purified synaptic vesicles and whole synaptosomes (Fig. 7). Intact synaptosomes were biotinylated using a non-permeant biotin derivative to label their plasma membrane. After mechanical disruption of the synaptosomes, biotinylated membranes were isolated on streptavidin-coated magnetic beads (B). As a control, non-biotinylated synaptosomes were treated in parallel (C). Synaptic vesicles (SV) with a high acetylcholine content were purified directly from *T. marmorata* electric organ by taking benefit of the much lower equilibrium density of acetylcholine filled vesicles, compared with depleted ones or endosomes (Diebler and Lazereg, 1985). As expected (Taubenblatt et al., 1999), the presynaptic membrane was enriched in the t-SNARE syntaxin-1 and depleted in synaptophysin, as compared to synaptic vesicles (Fig. 7); VAMP-2 was easily detected in both membranes (samples in Fig. 7 were adjusted to give bands of VAMP-2 of similar intensity). The a1 and c subunits of the V0 domain of V-ATPase were detected both in the synaptosomal and synaptic vesicle membranes (Fig. 7). This is in accordance with the c subunit immunogold detection in freeze-fractured synaptic vesicles and nerve terminal plasma membranes. We looked for subunits A and B of the catalytic V1 domain

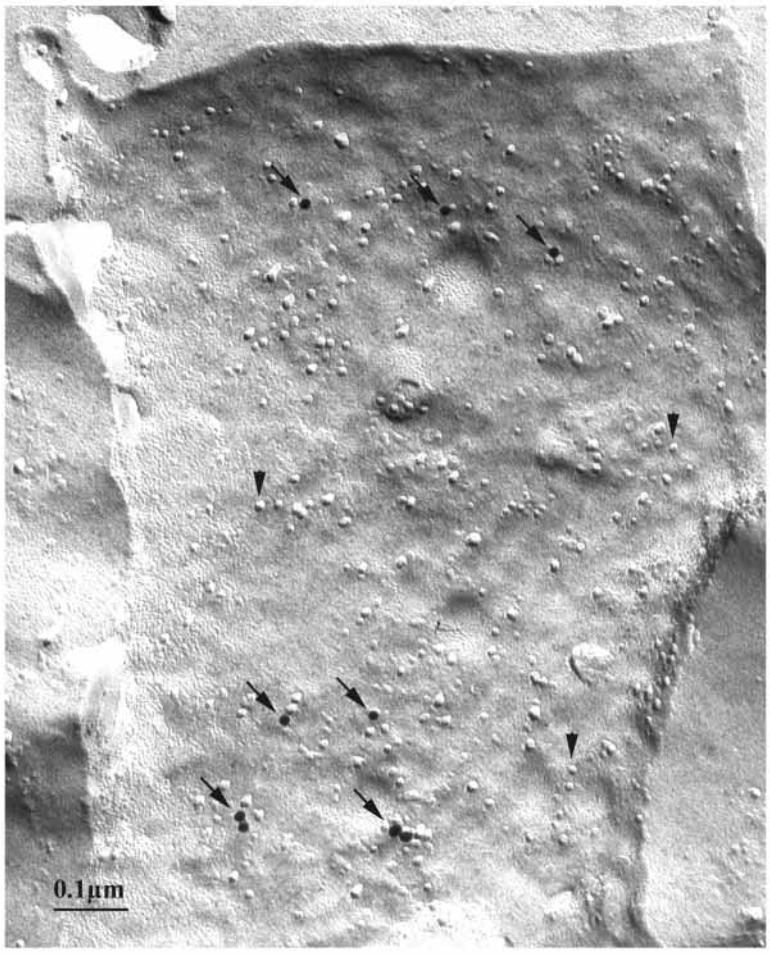


**Fig. 6.** V-ATPase c subunit is a constituent of large protein complexes. A flat surface of a freeze-fractured E face of a nerve terminal plasma membrane was labelled by anti-V-ATPase-c-subunit antibodies. Gold particles (15 nm, arrows) are preferentially associated with large intramembrane particles that correspond to large intramembrane proteins (arrowheads).

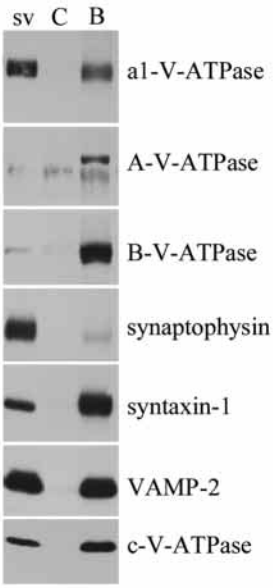


**Fig. 7.** Comparison of V-ATPase in the synaptosomal plasma membrane and synaptic vesicles. After biotinylation of intact synaptosomes, the biotinylated plasma membrane (B) was isolated on streptavidin-coated beads. Its antigenic content was compared with that of purified synaptic vesicles (sv). Samples were adjusted to contain similar VAMP-2 amounts. C, background binding of unbiotinylated synaptosomal membranes to streptavidin beads.

of V-ATPase (Fig. 7). These subunits were found associated with the synaptosomal plasma membrane, which therefore contains an entire V1V0-ATPase. They were absent from purified synaptic vesicles that only possess the V0 domain of V-ATPase. This very reproducible result was unexpected because synaptic vesicles, purified according to their high acetylcholine content, need an active V-ATPase to accumulate the neurotransmitter (Hicks and Parsons, 1992; Dolezal et al., 1993).

## V-ATPase membrane domain V0 interacts with SNARE complexes

Synaptosomal proteins were solubilized in non-denaturing conditions by the zwitterionic detergent CHAPS. Aliquots were incubated in parallel with monoclonal antibodies to SNARE proteins, covalently bound to agarose beads (Fig. 8A). The proportions of immunoprecipitated (ip) and unbound (nr) antigens were determined in each condition. The anti-VAMP-2 beads (19K2) bound most of the synaptosomal VAMP-2 (93±7%, *n*=3, mean±s.e.m. of *n* independent experiments), associated with at least half of syntaxin-1 (55±5%, *n*=3) and one-third of SNAP-25 (38±7%, *n*=3). Syntaxin-1 was efficiently precipitated by HPC1 beads (95±3%, *n*=4), in association with some SNAP-25 (31±3%, *n*=4) and VAMP-2 (20±2%, *n*=4). Taken together, this shows that 60% of syntaxin-1, 30-40% of SNAP-25 and 20% of VAMP-2 are engaged, under our conditions, in SNARE complexes.

Monoclonal antibody 1567 precipitated the three SNARE proteins, syntaxin-1 (61±3%, *n*=7), SNAP-25 (30±2%, *n*=7) and VAMP-2 (20±1%, *n*=7), in the proportions found in SNARE complexes (Fig. 8A). A second immunoprecipitation round was performed using synaptosomal protein samples that have been depleted of VAMP-2 or of syntaxin-1 (nr samples from 19K2 and HPC1 first precipitations, respectively; Fig. 8B). Under both sets of conditions, SNARE complexes should also have been removed. Beads coated with mAb 1567 could no longer precipitate syntaxin-1 and SNAP-25 in the absence of VAMP-2 (Fig. 8B, left), or SNAP-25 and VAMP-2 in the absence of syntaxin-1 (Fig. 8B, right). Therefore, mAb 1567 selectively binds the SNARE complexes without binding individual SNARE proteins. By contrast, the anti-syntaxin-1 antibody HPC1 still binds syntaxin-1 in the absence of VAMP, but not SNAP-25 (Fig. 8, left). In the absence of syntaxin-1, antibody 19K2 still precipitated VAMP-2 that was no longer in association with SNAP-25 (Fig. 8, right).

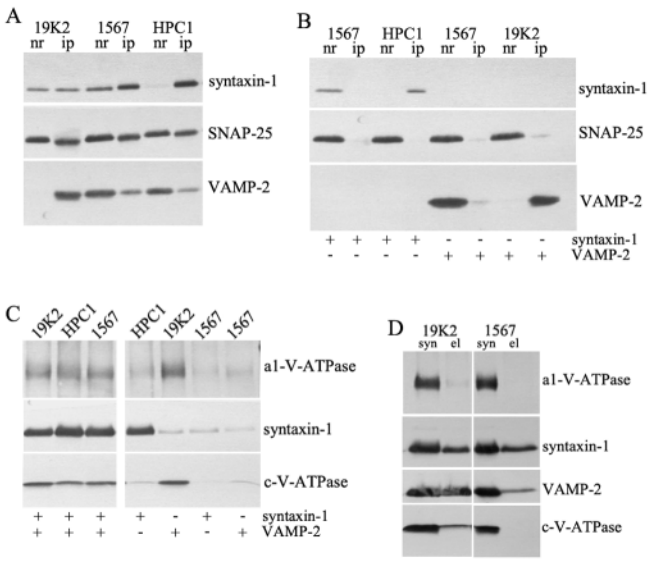


**Fig. 8.** Association of the V-ATPase membrane domain to SNARE complexes. (A) Solubilized synaptosomal proteins were incubated in parallel with different immunobeads, coated with mAbs to VAMP-2 (19K2), syntaxin-1 (HPC-1) and SNARE complexes (1567). The SNARE protein contents of immunoprecipitated (ip) and unbound (nr) samples deriving from 10 μg synaptosomal protein are compared. (B) Samples depleted of VAMP-2 (19K2 nr in A) or of syntaxin-1 (HPC-1 nr in A) were submitted to a second incubation with the immunobeads (as in A). The syntaxin-1, SNAP-25 and VAMP-2 contents of the resulting immunoprecipitated and unbound samples are compared (deriving from 20 μg synaptosomal protein). (C) Detection of the a1 and c subunits of V-ATPase in the immunoprecipitated samples deriving from the first incubation (left) or the second incubation after VAMP-2 or syntaxin-1 depletion (as indicated). Samples derive from 200 μg synaptosomal protein. (D) Parallel immunoprecipitations of VAMP-2 (19K2) or the SNARE complexes (1567) from solubilized synaptosomes (syn; 200 μg protein) or electric lobe homogenates (el; 2000 μg protein) as in (A).

In addition to the SNARE complexes, mAb 1567 also bound about 10% of both the synaptosomal V-ATPase a1 and c subunits (Fig. 8C, left). A similar result was obtained with the anti-VAMP-2 and the anti-syntaxin-1 immunobeads (Fig. 8C, left). The anti-SNARE complex mAb 1567 no longer precipitated the V0 subunits after depletion of VAMP-2 or syntaxin-1 (Fig. 8C, right). This demonstrates that this antibody does not bind directly to the V0 sector of V-ATPase, which was therefore precipitated via interactions with the SNARE complexes. After removal of syntaxin-1 and SNARE complexes, anti-VAMP-2 beads still retained some a1 and c subunits (Fig. 8C, right). In the VAMP-2-depleted samples, the V0 subunits were not pulled down with syntaxin-1 by the HPC1-coated beads (Fig. 8C, right). Therefore, the membrane domain of V-ATPase interacts with the v-SNARE VAMP-2, as previously reported by Galli et al. (Galli et al., 1996), but not

with the t-SNARE syntaxin-1. In addition, we have found that the membrane domain of V-ATPase interacts with the nerve terminal SNARE complexes. Using the anti-SNARE-complex mAb 1567, we estimated that 14±2% and 12±3% (five and six independent experiments) of the a1 and c subunits were in association with the SNARE complexes. Subunits A of the catalytic domain of V-ATPase were not detected with the V0 subunits (not shown), even after incubation of synaptosomes with DSP, dithiobis(succinimidyl propionate), a cross-linking agent that stabilizes association of the V1 and V0 domains (Morel et al., 1998). This shows that V-ATPase interactions with the SNARE complexes occur via the membrane domain. These results were obtained using the zwitterionic detergent CHAPS. When synaptosomal proteins were solubilized, in parallel to CHAPS experiments, by Triton X-100 or $C_{12}E_8$ (two non-ionic detergents), similar amounts of SNARE complexes were solubilized and immunoprecipitated. Triton X-100 and $C_{12}E_8$ were less efficient than CHAPS at solubilizing the V-ATPase proteolipid subunits and the amount of V0 subunits bound to the SNARE complexes was much lower after Triton X-100 or $C_{12}E_8$ solubilization (not shown).

We looked for SNARE complexes in electric lobes (Fig. 8D). Electric lobes and synaptosomes were solubilized in parallel by CHAPS and incubated with anti-VAMP (19K2) or anti-SNARE-complex (1567) immunobeads. Sample volumes were adjusted to incubate the beads with the same VAMP-2 and syntaxin-1 contents (Fig. 3). Similar amounts of VAMP-2 were recovered from the anti-VAMP immunobeads in both samples, part of which was associated with syntaxin-1 (Fig. 8D, 19K2) and SNAP-25 (not shown). Such SNARE complexes, less abundant in the electric lobes than in synaptosomes, were efficiently precipitated by mAb 1567 (Fig. 8D, 1567). Although synaptosomal SNARE complexes were associated with the a1 and c subunits of the V0 domain, these subunits were not detected in the electric lobe SNARE complex precipitates (Fig. 8D, 1567). Some c subunit was associated with VAMP-2 in the electric lobe sample, but in much lower amounts than in synaptosomes (Fig. 8D, 19K2). Notice that the electric lobe sample (1800 μg protein) contained ten times more V-ATPase c subunit than the synaptosome sample (200 μg protein; Fig. 3). The association of the V0 domain with SNARE complexes appears therefore to be restricted to nerve terminals and was not detected in the neuron cell bodies and dendrites.

We looked for an effect of synaptosome stimulation on the SNARE-complex/V0-domain interactions. Synaptosomes [2.5 (mg protein) $ml^{-1}$], under resting conditions (0.1 mM EGTA) or depolarized for 3 minutes by gramicidin D (10 μM) in the presence of 2 mM $Ca^{2+}$, were solubilized in parallel and SNARE complexes precipitated by the 1567 immunobeads. Under both conditions, the same amounts of SNARE complexes were recovered in association with similar quantities of the a1 and c V-ATPase subunits (not shown). Incubation of synaptosomes with concanamycin A, a specific inhibitor of V-ATPase that binds to the V0 domain (Huss et al., 2002), or *N*-ethyl-maleimide (which inhibits, among other enzymes, both the V-ATPase and NSF activities) did not modify recovery of SNARE complexes and their interactions with V0-V-ATPase. Therefore interactions of the membrane domain of V-ATPase with SNARE complexes appear to be independent of V-ATPase activity and of synaptosome stimulation.

## Discussion

In vertebrates, several genes encode different isoforms of the a subunit of V-ATPase, with tissue-specific expression (Toyomura et al., 2000; Nishi and Forgac, 2000; Mattson et al., 2000; Oka et al., 2001). We looked for mRNAs encoding the V-ATPase a subunits expressed in *T. marmorata* electric lobes by RT-PCR with degenerate primers. *T. marmorata* electric lobes contain a homogeneous population of 120,000 large neurons, the electromotoneurons, with few glial and endothelial cells (Fessard, 1958; Roberts and Ryan, 1975). Only one a-subunit isoform was amplified: the *T. marmorata* orthologue of the mouse a1 isoform. Three splice variants of the a1 subunit have been described in mice, according to the presence or absence of two small exons (Nishi and Forgac, 2000). In *T. marmorata* electric lobe, the major transcript corresponded to the a1-I variant, which contains the C-terminal exon. Minor transcripts that do not contain the C-terminal exon or contain the N-terminal one (a1-II) were also amplified from *T. marmorata* electric lobe mRNAs. No transcripts encoding other a-subunit isoforms were detected in spite of the fact that most of the V-ATPase in the neuronal cell bodies do not possess the subunit a1 isoform, regardless of the splice variant (see below). There could be two reasons for the failure to clone the somatodendrite-specific a-subunit isoform. First, we cannot exclude the possibility that the degenerate primers used in the RT-PCR cloning experiment failed to amplify it. Second, the somatodendrite-specific a-subunit isoform mRNAs might be too rare, compared with the nerve terminal ones, to be detected in the population of a-isoform RT-PCR fragments analysed. Actually, because each electromotoneuron has a huge nerve terminal arborization (in the electric organ) that has a 70 times larger volume than the neuronal cell body (estimated from our own data and data reviewed by Fessard, 1958), mRNAs encoding nerve terminal proteins must be much more abundant in the electric lobes than those coding for house-keeping somatic proteins.

Antibodies to the a1 isoform of the a-subunit were generated and used to study its tissue and subcellular distribution. This isoform was brain specific and not detected in liver and kidney, in accordance with the brain-specific expression of a1 transcripts in mammals (Nishi and Forgac, 2000; but see Toyomura et al., 2000), in contrast to the ubiquitous distribution of the proteolipid c subunit. Within neurons, the a1 isoform of the a subunit is enriched ten times in nerve terminals compared with neuron cell bodies and dendrites, enrichment that is similar to that of the nerve terminal specific proteins, VAMP-2 and syntaxin-1. V-ATPases associated to organelles in the electromotoneuron cell bodies, labelled by antibodies to the c subunit, therefore possess a different subunit a isoform. The specific targeting to nerve terminals of the a1 isoform of the V-ATPase a subunit suggests that it could carry a specific but unknown axonal sorting signal.

Within nerve terminals, using the SDS fracture-label technique (Fujimoto, 1995; Taubenblatt et al., 1999), the c subunit was found associated to synaptic vesicles, as expected (Hicks and Parsons, 1992; Morel et al., 1991). It was also detected in the presynaptic plasma membrane, associated with intramembrane particles that correspond to protein complexes with several transmembrane domains (Eskandari et al., 1998). This suggests that the proteolipid c subunit of V-ATPase is present in the presynaptic membrane as a constituent of a large

protein complex. In accordance with this, we have previously observed that, after synaptosome solubilization in non-denaturing conditions and velocity sedimentation, all V-ATPase c and d subunits migrated together in large (18S) protein complexes (Morel et al., 1998). It has been estimated from pharmacological data that one or two V-ATPase molecules are present per *T. marmorata* electric organ synaptic vesicle (Hicks and Parsons, 1992). Labelling of 20% of synaptic vesicles (see Results), each vesicle possessing two V-ATPase molecules, corresponds to a 10% efficacy in V0 V-ATPase immunogold labelling. Applied to the presynaptic plasma membrane, this would give a mean density of about 40 V-ATPase membrane domains per $\mu m^2$, with areas where the V-ATPase density could reach 200 molecules per $\mu m^2$.

The presence of the a1 and c subunits of the V-ATPase membrane sector in both the synaptic vesicle and presynaptic plasma membranes was confirmed using purified subcellular fractions. Their distribution is very similar to that of the v-SNARE VAMP-2, also present in both membranes (Taubenblatt et al., 1999). Classical synaptic vesicle proteins, including synaptophysin (Fig. 7) but also SV2 and the vesicular acetylcholine transporter (Taubenblatt et al., 1999), are present in the nerve terminal plasma membrane, albeit in much lower amounts than VAMP-2 (Taubenblatt et al., 1999) and V-ATPase membrane subunits. Therefore, whereas some V-ATPase molecules are probably transiently incorporated in the nerve terminal membrane in the course of the exo-endocytotic cycle of synaptic vesicles, in parallel to synaptophysin, most V-ATPase membrane domains have a more permanent presence in the presynaptic plasma membrane.

It was surprising to detect subunits of the catalytic sector (A and B subunits) bound to the isolated synaptosomal membrane and absent from the membrane of purified synaptic vesicles. This cannot be attributed to differences in the subunit composition of the V-ATPase V0 domains in synaptic vesicles and the presynaptic plasma membrane, which both contain the a1 isoform. Synaptic vesicles were purified by two successive centrifugations in sucrose density gradients, taking advantage of the much lower equilibrium density of vesicles that are filled with acetylcholine, compared with the density of depleted vesicles (Diebler and Lazereg, 1985). Because synaptic vesicles need an active V-ATPase to accumulate the neurotransmitter in vivo (Dolezal et al., 1993), it was surprising not to find the catalytic V1 domain associated with purified acetylcholine containing synaptic vesicles. One possibility would be that synaptic vesicle V-ATPase dissociates when the neurotransmitter content and/or the electrochemical proton gradient are maximal inside the organelle. In the presynaptic plasma membrane, where such large transmembrane gradients do not exist, V-ATPase molecules, at least part of them, would remain assembled. Downregulation of V-ATPase activity by reversible dissociation of the V1 sector from the membrane domain has been reported under different physiological conditions (Kane, 1995; Kane, 2000; Sumner et al., 1995). It should be stressed that V1 and V0 sectors are synthesized separately in the neuron cell body and transported in the axon at very different rates (Morel et al., 1998). They assemble when arrived in nerve terminals, to give an active V-ATPase (Morel et al., 1998). In isolated *T. marmorata* synaptosomes, two-thirds of the V1 sector is not associated with V0 in membranes (Morel et al., 1998). Dissociation of V-ATPase in vivo could be controlled both by the a-subunit isoform present in the V0 sector and by the cellular environment (Kawasaki-Nishi et al., 2001). Sorting of a special a-subunit isoform (a1-I) to the nerve terminal might have functional implications for regulation of the synaptic vesicle V-ATPase assembly and activity. In addition, fully assembled plasma membrane V-ATPases could participate in the regulation of the nerve terminal cytosolic pH by exporting protons in the synaptic cleft, as demonstrated for V-ATPases present in the macrophage plasma membrane (Swallow et al., 1990).

The V0 domain of V-ATPase interacts with the v-SNARE VAMP-2 and with SNARE complexes but not with the t-SNARE syntaxin-1. Association of VAMP-2 with the V-ATPase membrane domain has already been reported in rat brain solubilisates (Galli et al., 1996), but considered to exclude incorporation of VAMP-2 in SNARE complexes. This was not the case in our conditions because we co-precipitated the V-ATPase V0 domain with the SNARE complex whatever the anti-SNARE antibody we used. VAMP-2 is an abundant nerve terminal protein that is present in both synaptic vesicles and the presynaptic membrane (Taubenblatt et al., 1999). The presence in the same membrane of the three SNARE proteins allows the formation of cis-SNARE complexes as demonstrated in yeast vacuoles (Wickner and Haas, 2000). The abundance of such complexes is downregulated by the activity of the cytoplasmic ATPase NSF that promotes their dissociation (Wickner and Haas, 2000; Chen and Scheller, 2001; Jahn and Südhof, 1999). During nerve terminal fractionation, soluble NSF is removed and cis-SNARE complexes probably accumulate. Other SNARE complexes correspond to the trans-SNARE complexes that ensure synaptic vesicle docking to the presynaptic plasma membrane (Wickner and Haas, 2000; Chen and Scheller, 2001; Jahn and Südhof, 1999). Considering that only 5-10% of synaptic vesicles are apposed to the presynaptic membrane in *T. marmorata* synaptosomes, clearly a maximum of 5% of VAMP-2 molecules are expected to participate to trans-SNARE complexes. Therefore, of the 20% of VAMP-2 engaged in SNARE complexes with syntaxin-1 and SNAP-25, the remaining 15% of VAMP should be in cis-SNARE complexes. Most of the V0 domain that interacts with SNARE complexes should therefore correspond to presynaptic membrane V-ATPase V0 sectors in association with cis-SNARE complexes in the same membranes.

Exocytosis of synaptic vesicles during synaptic activity involves the tight docking of synaptic vesicles at special areas of the presynaptic plasma membrane, a process that requires the assembly of trans-SNARE complexes (Chen and Scheller, 2001; Jahn and Südhof, 1999). Upon calcium activation, a fusion pore opens, spanning the two apposed membranes and allowing the release of the synaptic vesicle neurotransmitter into the synaptic cleft. Fusion pores then either expand (leading to complete synaptic vesicle membrane fusion in the nerve terminal membrane) or close (leading to transmitter release without full fusion) (Alvarez de Toledo et al., 1993; Alés et al., 1999). The molecular nature of these fusion pores, made purely of lipids or lined by proteins, is still a matter of debate (Bruns and Jahn, 2002; Mayer, 2001; Zimmerberg, 2001). Several experimental lines of evidence suggest that the membrane sector of V-ATPase or its proteolipid ring could be such a

fusion pore (Peters et al., 2001; Morel et al., 2001). It is of interest to demonstrate here that the membrane domain of V-ATPase is present in both interacting membranes, the synaptic vesicle membrane and the presynaptic plasma membrane. Interactions with SNARE complexes could bring the V0 domain in strategic locations for exocytosis, favouring the formation of a V0-V0 trans-complex, the putative fusion pore, identified during yeast homotypic vacuole fusion (Peters et al., 2001). Finally, the existence of a special a-subunit isoform in nerve terminals might be important, not only for the proper targeting of the V-ATPase to the sites of transmitter storage and release but also for the regulation of the V-ATPase activity and, possibly, fusion pore formation.

We thank F.-M. Meunier for the gift of the *T. marmorata* electric lobe cDNA library and mRNAs, S. De la Porte and J. Barbier for fluorescence and confocal microscope facilities, respectively, and S. O'Regan for improving our manuscript. This work was supported by the Association de Recherche contre le Cancer (ARC grant #5941 to NM).

## References

**Alés, E., Tabares, L., Poyato, J. M., Valero, V., Lindau, M. and Alvarez de Toledo, G.** (1999). High calcium concentrations shift the mode of exocytosis to the kiss-and-run mechanism. *Nat. Cell Biol.* **1**, 40-44.

**Alvarez de Toledo, G., Fernandez-Chacon, R. and Fernandez, J. M.** (1993). Release of secretory products during transient vesicle fusion. *Nature* **363**, 554-558.

**Birman, S., Meunier, F.-M., Lesbats, B., le Caer, J. P., Rossier, J. and Israël, M.** (1990). A 15 kD proteolipid found in mediatophore preparations from *Torpedo* electric organ presents high sequence homology with the bovine chromaffin granule protonophore. *FEBS Lett.* **261**, 303-306.

**Bruns, D. and Jahn, R.** (2002). Molecular determinants of exocytosis. *Eur. J. Physiol.* **443**, 333-338.

**Chen, Y. A. and Scheller, R. H.** (2001). SNARE-mediated membrane fusion. *Nat. Rev. Cell Biol.* **2**, 98-106.

**Diebler, M.-F. and Lazereg, S.** (1985). Mg-ATPase and cholinergic synaptic vesicles. *J. Neurochem.* **44**, 1633-1641.

**Dolezal, V., Sbia, M., Diebler, M.-F., Varoqui, H. and Morel, N.** (1993). Effect of *N,N′*-dicyclohexylcarbodiimide on compartmentation and release of newly synthesized and preformed acetylcholine in *Torpedo* synaptosomes. *J. Neurochem.* **61**, 1454-1460.

**Eskandari, S., Wright, E. M., Kreman, M., Starage, D. M. and Zampighi, G. A.** (1998). Structural analysis of cloned plasma membrane proteins by freeze-fracture electron microscopy. *Proc. Natl. Acad. Sci. USA* **95**, 11235-11240.

**Fessard, A.** (1958). Les organes électriques. In *Traité de Zoologie*, Vol. 13 (Grassé, P. P., ed.), pp. 1143-1238. Ed. Masson, Paris, France.

**Fujimoto, K.** (1995). Freeze-fracture replica electron microscopy combined with SDS digestion for cytochemical labeling of integral membrane proteins. *J. Cell Sci.* **108**, 3443-3449.

**Füldner, H. and Stadler, H.** (1982). $^{31}$P-NMR analysis of synaptic vesicles. Status of ATP and internal pH. *Eur. J. Biochem.* **121**, 519-524.

**Galli, T., McPherson, P. S. and de Camilli, P.** (1996). The V0 sector of the V-ATPase, synaptobrevin and synaptophysin are associated on synaptic vesicles in a Triton X-100-resistant, freeze-thawing sensitive complex. *J. Biol. Chem.* **271**, 2193-2198.

**Gulik-Krzywicki, T. and Costello, M. J.** (1978). The use of low temperature X-ray diffraction to evaluate freezing methods used in freeze-fracture electron microscopy. *J. Microsc.* **112**, 103-113.

**Hicks, B. W. and Parsons, S. M.** (1992). Characterization of the P-type and V-type ATPases of cholinergic synaptic vesicles and coupling of nucleotide hydrolysis to acetylcholine transport. *J. Neurochem.* **58**, 1211-1220.

**Huss, M., Ingenhorst, G., Konig, S., Gassel, M., Dröse, S., Zeeck, A., Altendorf, K. and Wieczorek, H.** (2002). Concanamycin A, the specific inhibitor of V-ATPases, binds to V0 subunit c. *J. Biol. Chem.* **277**, 40544-40548.

**Jahn, R. and Südhof, T. C.** (1999). Membrane fusion and exocytosis. *Annu. Rev. Biochem.* **68**, 863-911.

**Kane, P. M.** (1995). Disassembly and reassembly of the yeast vacuolar $H^+$-ATPase in vivo. *J. Biol. Chem.* **270**, 17025-17032.

**Kane, P. M.** (2000). Regulation of V-ATPases by reversible disassembly. *FEBS Lett.* **469**, 137-141.

**Kawasaki-Nishi, S., Bowers, K., Nishi, T., Forgac, M. and Stevens, T.** (2001). The amino-terminal domain of the vacuolar proton-translocating ATPase a subunit controls targeting and in vivo dissociation, and the carboxyl-terminal domain affects coupling of proton transport and ATP hydrolysis. *J. Biol. Chem.* **276**, 47411-47420.

**Leng, X.-H., Manolson, M. F. and Forgac, M.** (1998). Function of the COOH-terminal domain of Vph1p in activity and assembly of the yeast V-ATPase. *J. Biol. Chem.* **273**, 6717-6723.

**Leng, X.-H., Nishi, T. and Forgac, M.** (1999). Transmembrane topography of the 100 kDa a subunit (Vph1p) of the yeast vacuolar proton-translocating ATPase. *J. Biol. Chem.* **274**, 14655-14661.

**Manolson, M. F., Wu, B., Proteau, D., Taillon, B. E., Roberts, B. T., Hoyt, M. A. and Jones, E. W.** (1994). *STV1* gene encodes functional homologue of 95 kDa yeast vacuolar $H^+$ATPase subunit Vph1p. *J. Biol. Chem.* **269**, 14064-14074.

**Mattson, J. P., Li, X., Peng, S.-B., Nilsson, F., Andersen, P., Lundberg, L. G., Stone, D. K. and Keeling, D. J.** (2000). Properties of three isoforms of the 116-kDa subunit of vacuolar H+-ATPase from a single vertebrate species. *Eur. J. Biochem.* **267**, 4115-4126.

**Mayer, A.** (2001). What drives membrane fusion in eukaryotes? *Trends Biochem. Sci.* **26**, 717-723.

**Michaelson, D. M. and Angel, I.** (1980). Determination of ΔpH in cholinergic synaptic vesicles: its effect on storage and release of acetylcholine. *Life Sci.* **27**, 39-44.

**Morel, N., Israël, M., Manaranche, R. and Mastour-Frachon, P.** (1977). Isolation of pure cholinergic nerve endings from *Torpedo* electric organ. *J. Cell Biol.* **75**, 43-55.

**Morel, N., Synguelakis, M. and le Gal la Salle, G.** (1991). Detection with monoclonal antibodies of a 15 kDa proteolipid in both presynaptic plasma membranes and synaptic vesicles in *Torpedo* electric organ. *J. Neurochem.* **56**, 1401-1408.

**Morel, N., Gérard, V. and Shiff, G.** (1998). Vacuolar $H^+$-ATPase domains are transported separately in axons and assemble in *Torpedo* nerve endings. *J. Neurochem.* **71**, 1702-1708.

**Morel, N., Dunant, Y. and Israël, M.** (2001). Neurotransmitter release through the V0 sector of V-ATPase. *J. Neurochem.* **79**, 485-488.

**Nelson, N. and Harvey, W. R.** (1999). Vacuolar and plasma membrane proton-adenosine triphosphatases. *Physiol. Rev.* **79**, 361-385.

**Nishi, T. and Forgac, M.** (2000). Molecular cloning and expression of three isoforms of the 100-kDa a subunit of the mouse vacuolar proton-translocating ATPase. *J. Biol. Chem.* **275**, 6824-6830.

**Nishi, T. and Forgac, M.** (2002). The vacuolar $H^+$-ATPases: Nature's most versatile proton pumps. *Nat. Rev.* **3**, 94-103.

**Oka, T., Murata, Y., Namba, M., Yoshimizu, T., Toyomura, T., Yamamoto, A., Sun-Wada, G.-H., Hamasaki, N., Wada, Y. and Futai, M.** (2001). a4, a unique kidney-specific isoform of mouse vacuolar $H^+$ ATPase subunit a. *J. Biol. Chem.* **276**, 40050-40054.

**Peters, C., Bayer, M. J., Bühler, S., Andersen, J. S., Mann, M. and Mayer, A.** (2001). Trans-complex formation by proteolipid channels in the terminal phase of membrane fusion. *Nature* **409**, 581-588.

**Roberts, B. L. and Ryan, K. P.** (1975). Cytological features of the giant neurons controlling electric discharge in the ray *Torpedo*. *J. Mar. Biol. Assoc. UK* **55**, 123-131.

**Schoonderwoert, V. T. G. and Martens, G. J. M.** (2001). Proton pumping in the secretory pathway. *J. Membrane Biol.* **182**, 159-169.

**Shiff, G., Synguelakis, M. and Morel, N.** (1996). Association of syntaxin with SNAP-25 and VAMP (synaptobrevin) in *Torpedo* synaptosomes. *Neurochem. Int.* **29**, 659-667.

**Stadler, H. and Tsukita, S.** (1984). Synaptic vesicles contain an ATP-dependent proton pump and show 'knob-like' protrusions on their surface. *EMBO J.* **3**, 3333-3337.

**Stevens, T. H. and Forgac, M.** (1997). Structure, function and regulation of the vacuolar $H^+$-ATPase. *Annu. Rev. Cell Dev. Biol.* **13**, 779-808.

**Sumner, J. P., Dow, J. A. T., Early, F. G. P., Klein, U., Jäger, D. and Wieczorek, H.** (1995). Regulation of plasma membrane V-ATPase activity by dissociation of peripheral subunits. *J. Biol. Chem.* **270**, 5649-5653.

**Swallow, C. J., Grinstein, S. and Rotstein, O. D.** (1990). A vacuolar type $H^+$-ATPase regulates cytoplasmic pH in murine macrophages. *J. Biol. Chem.* **265**, 7645-7654.

**Taubenblatt, P., Dedieu, J. C., Gulik-Krzywicki, T. and Morel, N.** (1999).

VAMP (synaptobrevin). is present in the plasma membrane of nerve terminals. *J. Cell Sci.* **112**, 3559-3567.

**Toyomura, T., Oka, T., Yamaguchi, C., Wada, Y. and Futai, M.** (2000). Three subunit a isoforms of mouse vacuolar $H^+$ATPase. *J. Biol. Chem.* **275**, 8760-8765.

**Wickner, W. and Haas, A.** (2000). Yeast homotypic vacuole fusion: a window on organelle trafficking mechanisms. *Annu. Rev. Biochem.* **69**, 247-275.

**Zimmerberg, J.** (2001). How can proteolipids be central players in membrane fusion? *Trends Cell Biol.* **11**, 233-235.